

Synthesis, X-ray crystal structure and spectroscopic characterization of the new dithiolene [Pd(Et₂timdt)₂] and of its adduct with molecular diiodine [Pd(Et₂timdt)₂·I₂·CHCl₃ (Et₂timdt = monoanion of 1,3-diethylimidazolidine-2,4,5-trithione)

Massimiliano Arca,^a Francesco Demartin,^b Francesco A. Devillanova,^{*a} Alessandra Garau,^a Francesco Isaia,^a Francesco Lelj,^c Vito Lippolis,^a Samuele Pedraglio^b and Gaetano Verani^a

^a Dipartimento di Chimica e Tecnologie Inorganiche e Metallorganiche, Via Ospedale 72, 09124 Cagliari, Italy. E-mail: devilla@vaxcal.unica.it

^b Dipartimento di Chimica Strutturale e Stereochimica Inorganica e Centro CNR, Via G. Venezian 21, 20133 Milano, Italy

^c Dipartimento di Chimica, Via N. Sauro 85, 85100 Potenza, Italy

Received 15th July 1998, Accepted 14th September 1998

The first Pd dithiolene [Pd(Et₂timdt)₂] **4a** belonging to the new class of metal dithiolenes deriving from the R₂¹timdt (R₂¹timdt = monoanion of 1,3-dialkylimidazolidine-2,4,5-trithione) ligand has been characterised by X-ray crystal structure determination on a single crystal [monoclinic, space group *P2₁/n*, *a* = 9.545(2), *b* = 5.417(2), *c* = 20.093(4) Å, β = 93.40(2)°, *Z* = 2], UV–VIS–NIR, diffuse solid state reflectance, FTIR, FT-Raman spectroscopies, solid state ¹³C NMR and cyclic voltammetry and the results have been comparatively discussed with those obtained for the analogous [Ni(Et₂timdt)₂] **4b**. The UV–VIS–NIR spectrum of **4a** is dominated by a very intense absorption band at 1010 nm (ε = 70 000 dm³ mol⁻¹ cm⁻¹). The NIR features of **4a** and **4b** have been examined on the basis of the electronic structure of their ground-state configurations, investigated by DFT calculations. The co-crystallisation of **4a** with I₂ yielded the [Pd(Et₂timdt)₂·I₂·CHCl₃] **6** adduct [monoclinic, space group *C2/m*, *a* = 21.724(9), *b* = 12.901(4), *c* = 11.004(6) Å, β = 102.83(4)°, *Z* = 4]. No short metal–metal interaction was observed in both **4a** and **6** (Pd···Pd 5.42 Å in **4a** and 5.25 Å in **6**), since each palladium ion is almost ‘sandwiched’ between two imidazolidine rings of parallel adjacent molecules.

In coordination chemistry metal dithiolenes represent a very interesting class of complexes. Because of their large π delocalization they exhibit uncommon properties, such as intense VIS–NIR absorption, high thermal and spectrochemical stability, and electrical conductivity.^{1–3} In addition they can exist in well defined oxidation states, neutral, mono- and di-anionic.⁴ Since the π electron delocalization involves the organic ligand atoms as well as the metal centre, these molecules have to be considered highly aromatic. In particular the frequency of the intense VIS–NIR absorption is assigned to a π → π* transition between HOMO and LUMO⁵ and depends on the nature of the substituents R¹ on the carbon atoms of the [S₂C₂R¹]₂²⁻ moiety. It has been shown that accepting substituents shift this absorption to lower energies⁵ compared with the value found for the so-called parent dithiolene [Ni(S₂C₂H₂)₂] (720 nm, ε = 14 000 dm³ mol⁻¹ cm⁻¹)^{6,7} where R¹ = H. Recently, some neutral Ni complexes belonging to the new class of metal dithiolenes [M(R₂¹timdt)₂] (R₂¹timdt = monoanion of 1,3-dialkylimidazolidine-2,4,5-trithione; R¹ = Et, Prⁱ, Bu) have been reported.⁸ These complexes are characterized by a very strong absorption at 1000 nm with absorption coefficient values up to 80 000 dm³ mol⁻¹ cm⁻¹ for [Ni(Prⁱ₂timdt)₂] (R¹ = Prⁱ, **4c**),⁹ the highest values ever observed in similar compounds. The closeness of this frequency to that of the Nd–YAG laser (excitation wavelength 1064 nm) makes these complexes very good candidates for technological applications, such as Q-switching¹⁰ for NIR-lasers or NIR dyes.⁵ With the aim to prepare complexes of this class having the NIR absorption as close as possible to the laser excitation energy, we first tried metal substitution as a synthetic tool. In this paper [Pd(Et₂timdt)₂] **4a**, the first Pd complex belonging to this new class of dithiolenes is fully characterized together with its analogue [Ni(Et₂timdt)₂] **4b**. In

order to obtain mixed-valence compounds of **4a**, which might have interesting conducting properties, we have reacted it with diiodine in several molar ratios, according to the same method successfully used for some Ni dithiolenes of the same class.⁹ Among the products, only [Pd(Et₂timdt)₂·I₂·CHCl₃] **6** has been characterized by X-ray diffraction and it is discussed in this paper.

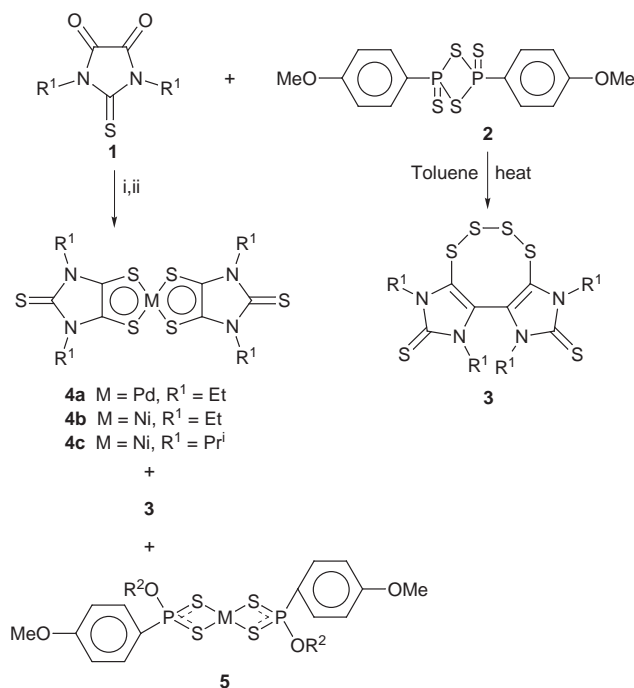
Experimental

All solvents and reagents were of the best Aldrich quality and were used as purchased. All operations were carried out under dry nitrogen atmosphere. Infrared spectra were recorded on a Bruker IFS55 spectrometer at room temperature. Polythene pellets with a Mylar beam-splitter and polythene windows (500–50 cm⁻¹, resolution 2 cm⁻¹) and KBr pellets with a KBr beam-splitter and KBr windows (4000–400 cm⁻¹, resolution 4 cm⁻¹) were used. FT-Raman spectra (resolution 4 cm⁻¹) were recorded on a Bruker RFS100 FT-Raman spectrometer, fitted with an In–Ga–As detector (room temperature) operating with a Nd–YAG laser (excitation wavelength 1064 nm) with a 180° scattering geometry. Electronic spectra (CHCl₃ solution; 20 °C) were recorded on a Cary 5 spectrophotometer. Diffuse reflectance measurements were recorded as KBr pellets. CP MAS solid state ¹³C NMR spectra were recorded on a Varian Unity Inova 400 MHz instrument operating at 100.5 MHz with samples packed into a zirconium oxide rotor. The ¹³C chemical shifts were calibrated indirectly through the adamantane peaks (δ 38.3, 29.2) related to SiMe₄. Cyclic voltammograms were recorded using an EG&G Model 273 at 25 °C in a Metrohm voltammetric cell with a combined working and counter platinum electrode and a standard Ag/AgCl (in 3.5 M KCl)

reference electrode (anhydrous CH_2Cl_2 ; sample concentration $1 \times 10^{-4} \text{ mol dm}^{-3}$; supporting electrolyte tetrabutylammonium tetrafluoroborate $1 \times 10^{-2} \text{ mol dm}^{-3}$). Cyclic voltammograms were recorded at scan rates ranging from 0.02 to 0.7 V s^{-1} . Density functional calculations^{11–13} were performed using the hybrid B3LYP functional^{14,15} with the Gaussian 94 package¹⁶ and the Shafer *et al.*¹⁷ VDZ basis set. The SCF procedure was performed on an optimized geometry starting from structural data, regularized in order to satisfy the D_{2h} symmetry. Calculations were performed on an IBM Risc 6000 550H, DECServer 4000 and on a SEH Pentium 133 MHz computer.

Synthesis

The synthesis of **4a** and **4b** can be accomplished either by metal halides or by metal powder (Scheme 1) as previously described.^{8,9}



Scheme 1 Reagents and conditions: i, Metal powder or metal halide, toluene, heat; ii, R²OH after concentration.

[Pd(Et₂timdt)₂] 4a. *Method (a).* A mixture of 1,3-diethylimidazolidine-2-thione-4,5-dione¹⁸ (**1**, R = Et; 1 g, 5.38 mmol), an equivalent amount of Lawesson's reagent (**2**) and a little excess of Pd powder was refluxed in anhydrous toluene (100 mL) for 8 h. The concentrated suspension was poured in about 100 mL of MeOH, from which, after 3 h at 4 °C, the solid was filtered, dried and extracted for 2 days with CHCl_3 in a Soxhlet apparatus (0.274 g, 18% yield).

Method (b). A stirred suspension of 1,3-diethylimidazolidine-2-thione-4,5-dione (**1**, R = Et; 0.50 g, 2.68 mmol), stoichiometric amounts of Lawesson's reagent (**2**), and PdCl_2 in 40 mL of toluene was refluxed for 30 min, concentrated under a nitrogen stream and poured in 40 mL of EtOH. The crystalline precipitate was separated (0.44 g, 61% yield). Needle-shaped dark crystals suitable for X-ray diffraction analysis were grown from a CHCl_3 - Me_3CN (2:1 v/v ratio) solution. Mp > 290 °C [Found (Calc. for $\text{C}_{14}\text{H}_{20}\text{N}_4\text{PdS}_6$): C, 31.0 (31.0); H, 3.8 (3.7); N, 10.2 (10.3); S, 35.2 (35.4)%]. Electronic spectrum in CHCl_3 : $\lambda(\epsilon)$ 274(60 600), 336(55 500), 510(11 440), 534(11 600), 654(4530), 746(4790), 1012nm (69 600 $\text{dm}^3 \text{ mol}^{-1} \text{ cm}^{-1}$). Solid state FTIR: ν/cm^{-1} 2973w, 2932w, 2869vw, 1444w, 1413vs, 1389vs, 1375vs, 1351vs, 1294vs, 1258vs, 1177m, 1152m, 1104s, 1081s, 976w, 954m, 807m, 752w, 567w, 428s, 410vw, 392m.

Raman spectrum (in the range 500–100 cm^{-1} ; relative intensities in parentheses, strongest = 10): ν/cm^{-1} 431(10), 341(7.2). Solid state ^{13}C NMR (atom labelling according to Fig. 1): δ 14.9 [C(12), C(12'), C(32), C(32')], 41.2 [C(11), C(11'), C(31), C(31')], 166.6 [C(4), C(4'), C(5), C(5')], 172.5 [C(2), C(2')].

[Ni(Et₂timdt)₂] 4b. This olive-green compound can be prepared from nickel powder (yield 20%) as previously reported.^{8,9} Mp 270 °C (decomp.) [Found (Calc. for $\text{C}_{14}\text{H}_{20}\text{N}_4\text{NiS}_6$): C, 33.6 (33.9); H, 4.1 (4.1); N, 11.1 (11.3); S, 38.8 (38.8)%]. Electronic spectrum in CHCl_3 : $\lambda(\epsilon)$ 262(17 800), 300(31 300), 340(42 110), 434(8660), 462(9165), 996 nm (76 500 $\text{dm}^3 \text{ mol}^{-1} \text{ cm}^{-1}$). Solid state FTIR: ν/cm^{-1} 2972w, 2961vw, 2932w, 2869vw, 1416s, 1391vs, 1376vs, 1350vs, 1288vs, 1255vs, 1180m, 1105s, 1081s, 977w, 953m, 809vw, 795w, 661w, 568w, 435s, 404vw, 390w, 378m. FT-Raman spectrum (in the range 500–100 cm^{-1} ; relative intensities in parentheses, strongest = 10): ν/cm^{-1} 435(6.1), 327(10), 139(3). Solid state ^{13}C NMR (atom labelling analogue to that used for **4a** in Fig. 1): δ 14.8, 14.0 [C(12), C(12'), C(32), C(32')], 41.8 [C(11), C(11'), C(31), C(31')], 162.5 [C(4), C(4'), C(5), C(5')], 169.8 [C(2), C(2')].

[Pd(Et₂timdt)₂]·I₂·CHCl₃ 6. A solution of **4a** (14 mg, $2.58 \times 10^{-5} \text{ mol}$) and I_2 (19 mg, $7.48 \times 10^{-5} \text{ mol}$) in CHCl_3 (40 mL) was slowly air evaporated. After a few days, dark needle-shaped crystals were separated and washed with light petroleum (bp 60–80 °C). Mp 260 °C (decomp.) [Found (Calc. for $\text{C}_{15}\text{H}_{21}\text{Cl}_3\text{I}_2\text{N}_4\text{PdS}_6$): C, 20.1 (19.7); H, 2.2 (2.3); N, 5.9 (6.1); S, 20.8 (21.0)%]. The spectroscopic features resemble those of **4a**.

Crystallography

A summary of the crystallographic data is given in Table 1. Data collections were performed on an Enraf-Nonius Cad-4 diffractometer. Lorentz, polarization and empirical absorption corrections¹⁹ were applied to the data. A linear correction for a slight decay, due to the loss of solvent molecules during data collection was also applied for **6**. All the hydrogen atoms, with the exception of that of the CHCl_3 molecule were introduced in the structure model and not refined. Scattering factors were taken from Cromer and Waber.²⁰ Anomalous dispersion effects were included in F_c ; the values for $\delta f'$ and $\delta f''$ were those of Cromer.²¹ All calculations were performed on a 80486/33 computer using Personal SDP software.²²

CCDC reference number 186/1161.

See <http://www.rsc.org/suppdata/dt/1998/3731/> for crystallographic files in .cif format.

Results and discussion

It has already been shown that cyclic pentaatomic vicinal dithiones are not isolable,^{23,24} therefore any conventional method of synthesis starting from them is not suitable for the preparation of $[\text{M}(\text{R}'_2\text{timdt})_2]$ dithiolenes. To overcome this obstacle, we have developed a one-step route leading to the complex **4** based on the sulfuration of 1,3-dialkylimidazolidine-2-thione-4,5-diones²⁵ (**1**) with Lawesson's reagent²⁶ (**2**) in the presence of a metal halide or metal powder (Scheme 1).^{8,9} However, the yields of these reactions are generally low owing to the formation of several by-products, among which the tetrathio-ceno derivatives²⁷ (**3**) and the *trans*-bis[*O*-alkyl (4-methoxyphenyl)phosphonodithioate²⁸ (**5**) have been identified. In the synthesis of Ni dithiolenes, the use of Ni powder leads to higher yields⁹ compared to NiCl_2 (yield for **4b**: 20% from Ni; 10% from NiCl_2). Surprisingly, in the synthesis of **4a** a very high yield is obtained using PdCl_2 as a starting material (yield 18% from Pd; 61% from PdCl_2).

Description of the structures of 4a and 6. Selected interatomic distances and angles for **4a** and its adduct with diiodine **6** are

Table 1 Crystallographic data for compounds **4a** and **6**

Compound	4a	6
Formula	C ₁₄ H ₂₀ N ₄ PdS ₆	C ₁₅ H ₂₁ Cl ₃ I ₂ N ₄ PdS ₆
<i>M</i>	543.13	916.31
Crystal system	Monoclinic	Monoclinic
Space group	<i>P2₁/n</i> (no. 14)	<i>C2/m</i> (no. 12)
<i>a</i> /Å	9.545(2)	21.724(9)
<i>b</i> /Å	5.417(2)	12.901(4)
<i>c</i> /Å	20.093(4)	11.004(6)
β /°	93.40(2)	102.83(4)
<i>V</i> /Å ³	1037.1(6)	3007(2)
<i>Z</i>	2	4
<i>T</i> /K	293(1)	293(1)
<i>D_c</i> /g cm ⁻³	1.74	2.02
μ (MoK α)/cm ⁻¹	14.7	33.3
Data/parameters ratio	1031/115	1272/154
Final <i>R</i> and <i>R_w</i> indices ^a	0.042, 0.043	0.053, 0.064
Min./max. height in final $\Delta\rho$ map/e Å ⁻³	-0.43(11)/0.61(11)	-0.65(13)/1.31(13)

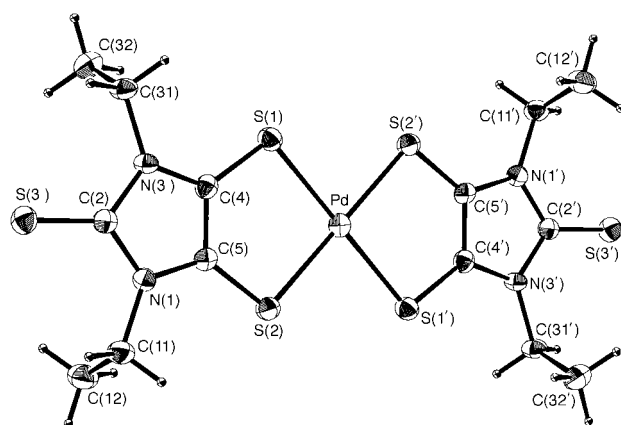
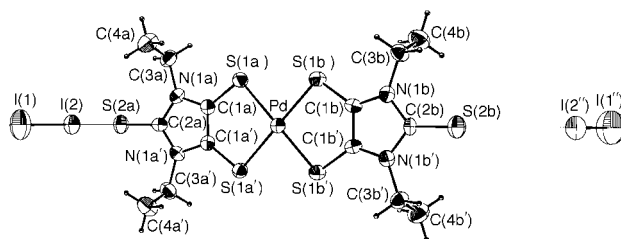
^a $R = [\sum(F_o - k|F_c|)/\sum F_o]$, $R_w = [\sum w(F_o - k|F_c|)^2/\sum wF_o^2]^{1/2}$.

Table 2 Selected interatomic distances (Å) and angles (°) for compounds **4a** and **6**

4a			
Pd–S(1)	2.295(2)	Pd–S(2)	2.294(2)
S(1)–C(4)	1.692(8)	S(2)–C(5)	1.687(8)
S(3)–C(2)	1.648(8)	C(4)–C(5)	1.397(9)
N(3)–C(4)	1.372(9)	N(1)–C(5)	1.367(8)
N(1)–C(2)	1.378(9)	N(3)–C(2)	1.394(9)
N(1)–C(11)	1.448(9)	N(3)–C(31)	1.466(9)
S(1)–Pd–S(2)	92.49(7)	S(1)–Pd–S(2')	87.51(7)
Pd–S(1)–C(4)	98.9(3)	Pd–S(2)–C(5)	99.4(3)
S(1)–C(4)–C(5)	125.0(6)	S(2)–C(5)–C(4)	124.2(6)
C(5)–N(1)–C(2)	110.7(6)	C(4)–N(3)–C(2)	109.8(6)
N(1)–C(5)–C(4)	107.1(7)	N(3)–C(4)–C(5)	107.2(7)
S(3)–C(2)–N(1)	127.1(6)	S(3)–C(2)–N(3)	127.6(6)
N(1)–C(2)–N(3)	105.3(6)		
6			
I(1)–I(2)	2.811(2)	I(2)–S(2a)	2.875(5)
Pd–S(1a)	2.287(3)	Pd–S(1b)	2.286(3)
S(1a)–C(1a)	1.697(9)	S(1b)–C(1b)	1.689(9)
S(2a)–C(2a)	1.740(15)	S(2b)–C(2b)	1.626(12)
N(1a)–C(1a)	1.382(10)	N(1b)–C(1b)	1.339(10)
N(1a)–C(2a)	1.327(10)	N(1b)–C(2b)	1.388(9)
C(1a)–C(1a')	1.343(19)	C(1b)–C(1b')	1.403(18)
S(2b)···I(2')	4.004(4)	I(1)···I(1'')	3.978(3)
S(1a)–Pd–S(1a')	93.0(1)	S(1b)–Pd–S(1b')	92.1(1)
S(1a)–Pd–S(1b)	87.4(1)	S(1a)–Pd–S(1b')	179.4(1)
Pd–S(1a)–C(1a)	97.9(3)	Pd–S(1b)–C(1b)	99.9(3)
S(1a)–C(1a)–C(1a')	125.6(3)	S(1b)–C(1b)–C(1b')	124.0(3)
N(1a)–C(1a)–C(1a')	107.5(5)	N(1b)–C(1b)–C(1b')	106.9(6)
C(1a)–N(1a)–C(2a)	107.5(9)	C(1b)–N(1b)–C(2b)	111.3(9)
N(1a)–C(2a)–N(1a')	109.9(12)	N(1b)–C(2b)–N(1b')	103.6(10)
S(2a)–C(2a)–N(1a)	125.0(6)	S(2b)–C(2b)–N(1b)	128.1(5)
I(1)–I(2)–S(2a)	179.6(1)	I(2)–S(2a)–C(2a)	98.3(5)
I(2'')···S(2b)–C(2b)	174.6(5)	I(1'')–I(2'')···S(2b)	88.3(1)
I(1'')···I(1)–I(2)	178.50(8)		

Symmetry codes: ' $-x, -y, -z$; " $1-x, -y, -z$; "' $2-x, -y, 1-z$.

given in Table 2. The molecular structure of **4a** is shown in Fig. 1. The molecule, which has an idealised *C_{2h}* symmetry, is located about a crystallographic inversion centre. The Pd atom displays a square planar coordination, which involves the two vicinal sulfur atoms of each of the two chelating ligands. The interatomic distances of the ring, compared with those previously reported for **4c**,⁹ are almost unaffected by the change of the metal. Differently from some other Pd and Pt dithiolenes, such as [Pd(S₂C₂H₂)₂] and [Pt(S₂C₂H₂)₂],^{29,30} where short metal–metal distances are found,³¹ no interaction is observed here

**Fig. 1** Molecular structure of complex **4a**.**Fig. 2** View of compound **6** showing the soft interaction with the iodine of another adduct. The chloroform molecule has been omitted.

(Pd···Pd 5.42 Å), but each Pd atom is almost 'sandwiched' between two imidazolidine rings of parallel adjacent molecules, with a metal–ring distance corresponding to an interplanar spacing of about 3.6 Å. The adduct **6** (shown in Fig. 2) has crystallographic *C_s* symmetry, with the Pd, C(2a), C(2b), S(2a), S(2b) and the diiodine atoms lying on the mirror plane. With the exception of the ethyl groups, the Pd complex is essentially planar; the Pd atom is only 0.008(1) Å out of its coordination plane, whereas the two pentaatomic metallacycles and the imidazolidine rings are exactly planar. The ethyl substituents in **6** are arranged in the same way as for **4a**. The complex molecule interacts with diiodine through the exocyclic sulfur atom S(2a) with an S(2a)–I(2) distance of 2.875(5) Å and induces a lengthening of 0.16 Å in the I–I bond with respect to solid I₂. This is a value similar to those found in the charge-transfer complexes of thiones with diiodine. In fact, the $d[\text{S}(2a)–\text{I}(2)]$ and $d[\text{I}(2)–\text{I}(1)]$ bond distances fit the correlation found for many charge-transfer complexes between sulfur donors and diiodine.³² The S(2b) atom, instead, is only involved in a soft

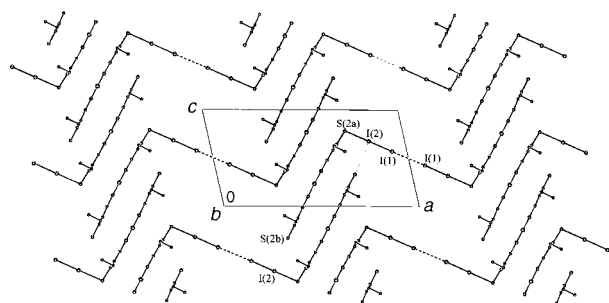


Fig. 3 Crystal packing of compound **6** seen along [010].

interaction with the iodine of another adjacent adduct [S(2b)⋯I(2^{''}) 4.004(4) Å]. As a result of the asymmetric interactions, the two imidazolidine moieties are significantly different. In particular C(2a)–S(2a) is about 0.1 Å elongated with respect to C(2b)–S(2b), and the two pentaatomic rings show differences both in the bond distances and in the angles, indicating a charge redistribution in the π system. In fact, the interatomic distances found in ligand (a) resemble those found in the adduct [Ni(Pr¹₂timdt)₂]₂·2.5I₂ 7⁹ [C(1a)–S(1a) 1.697(9) vs. 1.71(2) Å; C(1a)–C(1a') 1.34(2) vs. 1.33(4) Å; C(2a)–N(1a) 1.33(1) vs. 1.34(3) Å; S(2a)–I(2) 2.875(5) vs. 2.825(6) Å], in which both the terminal thioketonic sulfurs strongly interact with two different diiodine molecules, whereas the interatomic distances of the ligand (b) are close to those observed in **4a** (Table 2). The [Pd(Et₂timdt)₂]₂·I₂ adduct molecules are located about the crystallographic mirrors passing at $y = 0$, $y = 1$, etc., to form molecular layers stacked along [010]. Between these layers, there are clathrated chloroform molecules lying on the crystallographic mirror at $y = 0.5$. The pattern of the adduct molecules within each layer can be seen in Fig. 3: the complex molecules are arranged on parallel planes, with an interplanar distance of about 3.6 Å. The diiodine molecules are almost normal to these planes. The adduct molecules form rows running along [001], interconnected by I(1)⋯I(1) interactions of 3.978(3) Å. As for **4a**, the Pd atoms are 'sandwiched' between two imidazolidine rings of parallel adjacent molecules and again no short interaction is found between the Pd atoms (Pd⋯Pd 5.25 Å).

The CP MAS ¹³C NMR spectra recorded for **4a** and **4b** show the same features, the only difference being the slight splitting of the peaks assigned to the aliphatic carbons of **4b**. Unfortunately we have not been able to obtain structural data for **4b**, but this splitting may indicate a different orientation of ethyl groups compared to **4a**.

UV–VIS–NIR spectroscopy and DFT calculations

The most striking property observed in Ni dithiolenes deriving from the R¹₂timdt ligands is their very intense NIR-absorption. In chloroform solution, **4b** shows a very strong peak at 996 nm ($\epsilon = 76\,500\text{ dm}^3\text{ mol}^{-1}\text{ cm}^{-1}$), whereas the peak of **4a** is shifted in the desired direction at slightly but appreciably higher wavelengths (1010 nm, $\epsilon = 70\,000\text{ dm}^3\text{ mol}^{-1}\text{ cm}^{-1}$, Fig. 4). A remarkable difference appears in the visible region, due to the different position of the d–d bands. As a consequence, while Ni dithiolenes are olive-green, the new Pd dithiolene is purple. The position of the NIR band is unchanged in the solid state, as shown by diffuse reflectance measurement, and the spectral properties of compound **6** in the solid state are the same as for **4a**. The characteristic VIS–NIR band has been the subject of many studies^{4,33,34} in related simpler compounds and has been generally assigned to a π – π^* transition. In view of a better understanding of the nature of the absorption, a DFT approach using a hybrid functional has been used. Hybrid-DFT computations have been shown to work nicely with transition metals³⁵ both in the ground state and in the excited state.³⁶ To understand the effect of the R¹₂timdt bulky ligand, the calculations have been performed both on the parent [Ni(S₂C₂H₂)₂]

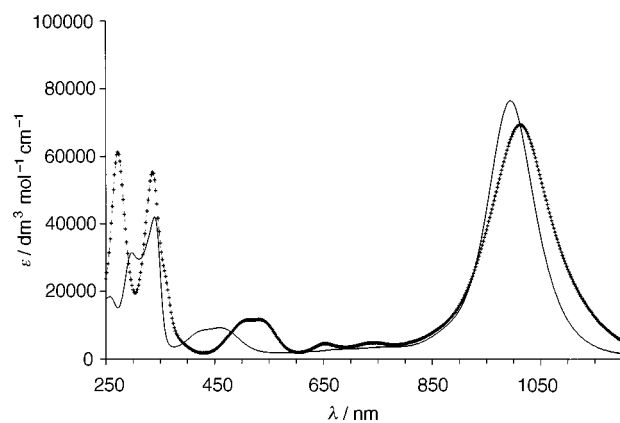


Fig. 4 UV–VIS–NIR spectra of compounds **4a** (+) and **4b** (—) measured in chloroform at 20 °C.

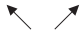
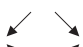




and the hypothetical [Ni(H₂timdt)₂] (R¹ = H) dithiolenes. The calculation of the electronic structure and energy of the parent [Ni(S₂C₂H₂)₂] dithiolene describes the ground state as ¹A_g. The HOMO (b_{1u}) is a π orbital built by the four p_z sulfur AOs (assuming the molecule is disposed in the xy plane) and the four p_z carbon AOs taken with opposite phases. As obvious in a B_{1u} irreducible representation, the d orbitals of the metal do not give any contribution to the HOMO; besides metal participates in this MO with its virtual 4p_z orbital. The LUMO (b_{2g}) π^* orbital, instead, is fully delocalized on the whole set of atoms of the molecule and involves the nickel atom through the 3d_{xz} orbital. The Ni atom bears a slight positive Mulliken charge (+0.017 e), opposite in sign even though not very different from the previous simple HF result (–0.07 e).³⁷ These results confirm the trend previously obtained³⁵ by the semi-empirical INDO³⁸ method.

In [Ni(H₂timdt)₂], the HOMO and LUMO in the ground state (¹A_g) belong to the same b_{1u} and b_{2g} representations, as found in the parent dithiolene. While the p_z orbitals of the exocyclic sulfurs are involved both in the HOMO and in the LUMO, those of the nitrogen atoms participate only in the HOMO. Again, the metal contributes to the LUMO only with its 3d_{xz} orbital. As in the case of the parent compounds, our calculations confirm the attribution of the intense NIR band to a π – π^* transition. According to a Mulliken population, a positive charge is concentrated on the metal atom (+0.101 e) and on the carbon atoms [+0.022 e for those of the dithiolene system and +0.072 e for the carbon (2)]. The donor sulfur atoms are negatively charged (–0.058 e) as well as the thioketonic terminal sulfurs (–0.205 e). The nitrogen atoms bring a –0.067 e negative charge. As far as the energies involved in the NIR transition are concerned, since Koopman's theorem is not valid for DFT calculations, the Kohn–Sham orbital energies cannot be used as in the case of HF calculations. Nevertheless, the energy difference, ΔE , between HOMO and LUMO orbitals can be used as a significant parameter. Thus, it can be noted that, according to the experimentally observed trend, the ΔE value decreases from 15 500 cm^{–1} in the parent dithiolene to 9100 cm^{–1} in **4b**. The very close value found for **4a** is easily explained when one observes that the metal contribution to the orbitals involved in the transition is indeed very small. However, the substitution of Ni by Pd has shifted the band 14 cm^{–1} in the desired direction.

Vibrational spectroscopy

Neglecting the possible conformations of the arms in the [M(R¹₂timdt)₂] unit, the molecule belongs to the D_{2h} point group, where the stretching normal modes of the MS₄ unit belong to the A_g, B_{1g}, B_{2u} and B_{3u} and the bending normal modes to 2B_{1g}, B_{3u} and B_{2u} representations. In Table 3 the most important

Table 3 Experimental vibrational frequencies (500–50 cm⁻¹) for compounds **4a** and **4b** compared with those calculated for [Ni(H₂timdt)₂]

	Mode	Calculated frequencies/cm ⁻¹	Experimental frequencies/cm ⁻¹	
			4a	4b
Raman active modes	 a _g stretching	317	341	327
	 a _g bending	446	431	435
	 b _{1g} bending	442		
FIR active modes	 b _{3u} stretching	366	392	378
	 b _{2u} stretching	373		
	 b _{3u} bending	435	428	435

calculated and experimental vibrations are summarized. The even modes are Raman active and are resonance enhanced by the NIR absorption both for **4a** and **4b**,⁹ as these compounds strongly absorb in the region of the Nd-YAG laser source. The FT-Raman spectra of **4a** and **4b** are dominated by two peaks both in solution and in the solid state, although spectra of better quality are obtainable in solution (341 and 431 cm⁻¹ for **4a**, 327, 435 cm⁻¹ for **4b**). While the first peak can be assigned to the a_g stretching mode, calculated at 317 cm⁻¹ for [Ni(H₂timdt)₂], the second one might be assigned to a_g or to the b_{1g} bending modes, calculated at 446 and 442 cm⁻¹ respectively. The lower frequency band shifts on passing from **4a** to **4b** as observed for [Pd(mnt)₂]²⁻ and [Ni(mnt)₂]²⁻ [mnt = C₂S₂(CN)₂] (349 and 335 cm⁻¹ respectively),³⁹ probably as a consequence of the increased metal-d/ligand-π orbital overlap, which overcomes the expected mass effect.³⁷ In the FIR region the bands having the highest calculated intensities in the Ni model compound fall at 435 (bending b_{3u}), 373 (stretching b_{2u}) and 366 cm⁻¹ (stretching b_{3u}) with calculated relative intensities of 236, 11 and 10 respectively. In the experimental FIR spectrum of **4b** two bands are present at 435 vs and 378 m cm⁻¹. These bands shift to 428 vs and 392 m cm⁻¹ in **4a**. In the MIR region the spectra of **4a** and **4b** are almost indistinguishable, all the observed bands being related to the same organic framework.

Electrochemistry

Cyclic voltammograms in CH₂Cl₂ have already been reported for **4b** and **4c**.^{8,9} Analogously, **4a** is characterized under the same experimental conditions by two reversible monoelectronic reductions ($E_{1/2}^1 = +0.05$ and $E_{1/2}^2 = -0.31$ V vs. Ag/AgCl in 3.5 M KCl) and a two electron oxidation. This process is more reversible than in the case of **4b** and **4c** and in this case the cathodic peak is visible and well defined ($E_{pa}^3 = +0.88$ V, $\Delta E = 0.26$, scan rate = 100 mV s⁻¹). The cyclic voltammetric curves of **4a** and **4b** are shown in Fig. 5. It should be noted that the reduction potentials of the Pd derivative are higher than those of the Ni complex, while the oxidation anodic peak occurs at about the same potential. On the basis of previous observations the reduction processes can be assigned to the formation of the two anionic forms of the dithiolene **4a**, namely [Pd(Et₂timdt)₂]⁻ and [Pd(Et₂timdt)₂]²⁻, while the oxidation process is probably related to the oxidation of the ligand, as previously pointed out for **4c** for which a mixed-valence

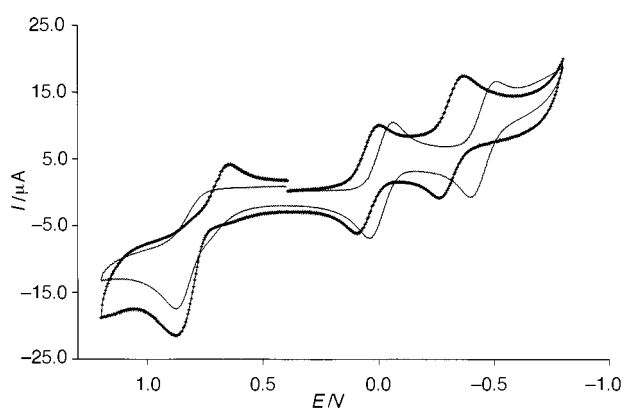


Fig. 5 Cyclic voltammetric response recorded at a platinum electrode on an anhydrous CH₂Cl₂ solution of complexes **4a** (+) and **4b** (—) (reference Ag/AgCl in 3.5 M KCl; supporting electrolyte NBu₄BF₄; scan rate 0.100 V s⁻¹).

compound containing the oxidized [Ni(Pr¹timdt)₂I₂] unit was identified by X-ray crystal structure determination.⁹ DFT calculations, indicating that the metal contributes to the LUMO through its nd_{xz} orbital and to the HOMO only through its virtual (n + 1)p_z orbitals, account for the almost identical oxidation potentials and for the shifts in the reduction processes for **4a** and **4b**. It is interesting to compare the redox properties of this new class of complexes with those of the dithiolenes deriving from the dmit ligand (dmit = 4,5-dimercapto-1,3-dithiole-2-thionate, C₃S₅²⁻)⁴⁰ in which two sulfur atoms are present instead of the NR¹ groups. In the case of the nickel derivative the reduction in MeCN from the neutral to the monoanionic form is irreversible and is observed at a value of +0.22 V vs. Ag/AgCl, determined by differential pulse polarography, extrapolating to a scan rate of 0 mV s⁻¹.⁴¹ The reduction to the bianionic form is reversible ($E_{1/2} = -0.13$ V vs. Ag/AgCl),⁴¹ and the difference in the potential between the two processes is almost the same as observed for **4b**. These features account for the different stabilities of the neutral forms of [M(R¹timdt)₂] and [M(dmit)₂]. The cyclic voltammogram of [Pd(dmit)₂]⁻ dithiolene in MeCN is similar to that of the Ni analogue, with the anodic peaks merging into a single broader peak.⁴² No oxidation process to a cationic form is observed in the Ni and Pd dmit derivatives⁴⁰ whereas an irreversible oxidation similar to

that observed in **4a**, **4b** and **4c** was previously found for other dithiolenes, such as $[\text{Ni}(\text{ddd})_2]$ (ddd = 5,6-dihydro-1,4-dithiin-2,3-diselenolate, $\text{C}_4\text{H}_4\text{S}_2\text{Se}_2$) and $[\text{Ni}(\text{dddt})_2]$ (dddt = 5,6-dihydro-1,4-dithiin-2,3-dithiolate, $\text{C}_4\text{H}_4\text{S}_4$), $E_{\text{pa}} = +0.71$ and $+0.99$ V respectively vs. Ag/AgCl in PhCN.⁴³

Conclusions

In view of obtaining new materials for Q-switching laser applications, spectrochemically stable molecules having an intense absorption near to the laser excitation energy are needed.⁵ The new class of dithiolenes $[\text{M}(\text{R}'_2\text{timdt})_2]$ is therefore very promising, respecting those requirements. With respect to the previously reported Ni-dithiolenes,⁸ the new $[\text{Pd}(\text{Et}_2\text{timdt})_2]$ complex (**4a**) shows a slight shift of the $\pi-\pi^*$ transition towards lower energy. Therefore the position of the NIR band of this compound (1010 nm, $\epsilon = 70000 \text{ dm}^3 \text{ mol}^{-1} \text{ cm}^{-1}$) makes it more suitable for applications with the Nd-YAG laser (1064 nm). As previously pointed out, this type of dithiolenes might be also interesting conducting materials if mixed-valence compounds would be synthesized. Therefore we have attempted the reaction of **4a** with I_2 , but so far only the 1:1 adduct **6** has been structurally characterized. Both in the crystal structure of **4a** and **6**, the dithiolene units are stacked in a tilted orientation with each palladium ion almost 'sandwiched' between two planar imidazolidine rings of the parallel adjacent molecules. In the adduct structure each Pd dithiolene molecule interacts with a diiodine molecule through the thio-ketonic sulfur of one side, the corresponding sulfur of the other ring being involved only in a soft interaction with the iodine of another adduct. The spectroscopic properties of **4a** and of its Ni analogue **4b** are very similar, as proved by UV-VIS-NIR (both in the solid state and in solution), FTIR, FT-Raman and CP MAS ¹³C NMR spectroscopies. Electrochemical measurements demonstrate that for **4a** oxidation over the neutral state is achievable and quasi-reversible, differentiating it both from the Ni analogue **4b**, where this oxidation is irreversible and from $[\text{Ni}(\text{dmit})_2]$ ⁴⁰ in which no oxidation process is detected.

References

- 1 J. R. Ferraro and J. M. Williams, *Introduction to Synthetic Electrical Conductors*, Academic Press, New York, 1987; T. Nakamura, A. E. Underhill, A. T. Coomber, R. H. Friend, H. Tajima, A. Kobayashi and H. Kobayashi, *Inorg. Chem.*, 1995, **34**, 870.
- 2 J. A. McCleverty, *Prog. Inorg. Chem.*, 1968, **10**, 49; A. Sato, H. Kobayashi, T. Naito, F. Sakai and A. Kobayashi, *Inorg. Chem.*, 1997, **36**, 5262; A. E. Pullen, S. Zeltner, R. M. Olk, E. Hoyer, K. A. Abboud and J. R. Reynolds, *Inorg. Chem.*, 1997, **36**, 4163 and refs. therein.
- 3 U. T. Mueller-Westerhoff, B. Vance and D. I. Yoon, *Tetrahedron*, 1991, **47**, 909; M. Bousseau, L. Valade, J. P. Legros, P. Cassoux, M. Garbouskas and L. V. Interrante, *J. Am. Chem. Soc.*, 1986, **108**, 1908; A. Kobayashi, H. Kim, Y. Sasaki, K. Murata, R. Kato and H. Kobayashi, *J. Chem. Soc., Faraday Trans.*, 1990, **86**, 361.
- 4 R. Williams, E. Billig, J. H. Waters and H. B. Gray, *J. Am. Chem. Soc.*, 1966, **88**, 43.
- 5 U. T. Mueller-Westerhoff and B. Vance, *Comp. Coord. Chem.*, 1987, **2**, 595; D. I. Yoon, PhD Thesis, University of Connecticut, 1988.
- 6 K. W. Browall and L. V. Interrante, *J. Coord. Chem.*, 1973, **3**, 27.
- 7 G. N. Schrauzer and V. P. Mayweg, *J. Am. Chem. Soc.*, 1965, **87**, 3585.
- 8 F. Bigoli, P. Deplano, F. A. Devillanova, V. Lippolis, P. J. Lukes, M. L. Mercuri, M. A. Pellinghelli and E. F. Trogu, *J. Chem. Soc., Chem. Commun.*, 1995, 371.
- 9 F. Bigoli, P. Deplano, F. A. Devillanova, J. R. Ferraro, V. Lippolis, P. J. Lukes, M. L. Mercuri, M. A. Pellinghelli and E. F. Trogu, *Inorg. Chem.*, 1997, **36**, 1218.
- 10 K. H. Drexage and U. T. Mueller-Westerhoff, *IEEE J. Quantum*

- Electron*, 1972, **QE-8**, 759; *US Pat.*, 3 743 964, 1973; P. N. Prasad and D. J. Williams, *Introduction to Non-linear Optical Effects in Molecules and Polymers*, Wiley, New York, 1991, p. 222.
- 11 J. Labanowsky and J. Andzelm, *Density Functional Methods in Chemistry*, Springer-Verlag, New York, 1991.
- 12 T. Ziegler, *Chem. Rev.*, 1991, **91**, 651 and refs. therein.
- 13 A. C. Scheiner, J. Baker and J. W. Andzelm, *J. Comput. Chem.*, 1997, **18**, 775.
- 14 A. D. Becke, *J. Chem. Phys.*, 1993, **98**, 1372; 5648.
- 15 C. Lee, W. Yang and R. G. Parr, *Phys. Rev. B*, 1988, **37**, 785.
- 16 Gaussian 94 (Revision D.1 & E.1), M. J. Frisch, G. W. Trucks, H. B. Schlegel, P. M. W. Gill, B. G. Johnson, M. A. Robb, J. R. Cheeseman, T. A. Keith, G. A. Petersson, J. A. Montgomery, K. Raghavachari, M. A. Al-Laham, V. G. Zakrzewski, J. V. Ortiz, J. B. Foresman, C. Y. Peng, P. Y. Ayala, M. W. Wong, J. L. Andres, E. S. Replogle, R. Gomperts, R. L. Martin, D. J. Fox, J. S. Binkley, D. J. Defrees, J. Baker, J. P. Stewart, M. Head-Gordon, C. Gonzalez and J. A. Pople, Gaussian, Inc., Pittsburgh PA, 1995.
- 17 A. Schafer, H. Horn and R. Ahlrichs, *J. Chem. Phys.*, 1992, **97**, 2571.
- 18 P. J. Stoffel, *J. Org. Chem.*, 1964, **29**, 2794.
- 19 A. C. North, D. C. Phillips and F. S. Mathews, *Acta Crystallogr., Sect. A*, 1968, **24**, 351.
- 20 D. T. Cromer and J. T. Waber, *International Tables for X-Ray Crystallography*, The Kynoch Press, Birmingham, 1974, vol. IV, Table 2.2B.
- 21 D. T. Cromer, *International Tables for X-Ray Crystallography*, The Kynoch Press, Birmingham, 1974, vol. IV, Table 2.3.1.
- 22 B. Frenz, *Comp. Phys.*, 1988, **2**, 42; *Crystallographic Computing*, Oxford University Press, 1991, p. 126.
- 23 H. W. Roesky, H. Hofman, W. Clegg, M. Noltemeyer and G. M. Sheldrick, *Inorg. Chem.*, 1982, **21**, 3798.
- 24 R. Isaksson, T. Liljefors and J. Sandstrom, *J. Chem. Res. (S)*, 1981, 43.
- 25 P. J. Stoffel, *J. Org. Chem.*, 1964, **29**, 2794.
- 26 S. Sheibe, B. J. Pedersen and S.-O. Lawesson, *Bull. Soc. Chim. Belg.*, 1978, **87**, 229.
- 27 F. Bigoli, M. A. Pellinghelli, D. Atzei, P. Deplano and E. F. Trogu, *Phosphorus Sulfur*, 1987, **37**, 189.
- 28 M. Arca, A. Cornia, F. A. Devillanova, A. C. Fabretti, F. Isaia, V. Lippolis and G. Verani, *Inorg. Chim. Acta*, 1997, **262**, 81.
- 29 S. Alvarez, R. Vicente and R. Hoffmann, *J. Am. Chem. Soc.*, 1985, **107**, 6253.
- 30 K. W. Browall and L. V. Interrante, *J. Coord. Chem.*, 1973, **3**, 27.
- 31 K. W. Browall, L. V. Interrante and J. S. Kasper, *Inorg. Chem.*, 1972, **11**, 1800.
- 32 P. Deplano, F. A. Devillanova, J. R. Ferraro, F. Isaia, V. Lippolis and M. L. Mercuri, *Appl. Spectrosc.*, 1992, **46**, 1625 and refs. therein.
- 33 S. I. Shupack, I. Billig, R. J. H. Clark, R. Williams and H. B. Gray, *J. Am. Chem. Soc.*, 1964, **86**, 4594.
- 34 Z. S. Herman, R. F. Kirchner, G. H. Loew, U. T. Mueller-Westerhoff, A. Nazzari and M. C. Zerner, *Inorg. Chem.*, 1982, **21**, 46.
- 35 C. Adamo and F. Lejl, *J. Chem. Phys.*, 1995, **103**, 10605; F. Lejl, C. Adamo and V. Barone, *Chem. Phys. Lett.*, 1994, **230**, 189.
- 36 C. Daul, *Int. J. Quantum Chem.*, 1994, **52**, 867.
- 37 I. Fischer-Hjalmars and A. Henriksson-Enflo, *Int. J. Quantum Chem.*, 1980, **18**, 409; D. Demoulin, I. Fischer-Hjalmars, A. Henriksson-Enflo, J. A. Pappas and M. Sandbom, *Int. J. Quantum Chem.*, 1977, **12** (Suppl. 1), 351.
- 38 J. A. Pople, D. Beveridge and P. Dobosh, *J. Chem. Phys.*, 1967, **47**, 2026.
- 39 R. J. H. Clark and P. C. Turtle, *J. Chem. Soc., Dalton Trans.*, 1977, 2142.
- 40 G. Steimecke, H. J. Sieler, R. Kirmse and E. Hoyer, *Phosphorus Sulfur*, 1979, **7**, 49.
- 41 R. Kato, H. Kobayashi, A. Kobayashi and Y. Sasaki, *Bull. Chem. Soc. Jpn.*, 1986, **59**, 627.
- 42 B. Pomarède, B. Garreau, I. Malfant, L. Valade, P. Cassoux, J. P. Legros, A. Audouard, L. Brossard, J. P. Ulmet, M. L. Doublet and E. Canadell, *Inorg. Chem.*, 1994, **33**, 3401.
- 43 H. Fujiwara, E. Arai and H. Kobayashi, *Chem. Commun.*, 1997, 837.

Paper 8/05494K